

## Carboxylic Carbon Nanotube: Catalyst Support Material and Oxygen Reduction Reaction of Microbial Fuel Cells

Nengwu Zhu<sup>1,2,\*</sup>, Jianjian Huang<sup>1</sup>, Weihang Shen<sup>1</sup>, Lixing Tu<sup>1</sup>, Pingxiao Wu<sup>1,2</sup>, Haiqin Ma<sup>1</sup>

<sup>1</sup> School of Environment and Energy, South China University of Technology, Guangzhou 510006, China

<sup>2</sup> Key Laboratory of Pollution Control and Ecosystem Restoration in Industry Clusters, Ministry of Education, Guangzhou 510006, China

\*E-mail: [nwzhu@scut.edu.cn](mailto:nwzhu@scut.edu.cn)

Received: 16 November 2014 / Accepted: 3 December 2014 / Published: 19 January 2015

---

The catalyst support materials (CSMs) greatly affect the catalytic efficiency and performances of microbial fuel cells (MFCs). The purpose of this study is to evaluate the effect of prepared CSMs on oxygen reduction reaction (ORR) at the air cathode of MFCs. Membrane free single-chamber air cathode MFCs, M80 and M95, are constructed using carboxylic modified carbon nanotube (CNTs) prepared under different conditions as the CSMs. The Experimental results show that comparing with MPT (the control) containing Pt/C as catalyst, which gains a maximum power density of 447.29mW/m<sup>2</sup>, the M80 achieves a maximum power density of 773.9 mW/m<sup>2</sup>, Noticeably, the M95 increases the power density to 911.3 mW/m<sup>2</sup>. Moreover, the internal resistance is decreased by 67% to 310Ω of M95 and 44% to 359Ω of M80 comparing with MPT(518Ω). Besides, From the polarization curves, open circuit voltages are 0.735V and 0.776V for M80 and M95 which is higher than MPT with 0.621V. X-ray photoelectron spectroscopy, X-ray diffraction and scanning electron microscope analysis demonstrate that the higher efficiency of Pt/CNT-2 catalyst may be attributable to the richer O, N and S-containing groups on the surface of CSM CNT-2 under higher temperature treatment.

---

**Keywords:** microbial fuel cell; carbon nanotube; carboxylic; catalyst support materials; oxygen reduction reaction

### 1. INTRODUCTION

Microbial fuel cells (MFCs), known as emerging technologies, can generate electricity directly from oxidation of biodegradable organic and inorganic matters [1-3]. Such environmental-friendly devices can achieve power generation at the same time to treating wastewater, This is the most important characteristics of MFCs [4]. Thus, MFCs attracted worldwide interests under the conditions of environmental pollution and energy dilemma [5].

Actually, in the infancy stage, MFCs could only generate pretty weak power. With the occurrence of exo-mediatorless MFCs [6], great efforts have been sacrificed to the power enhancement of MFCs. Nowadays, it is considered that the power generated by MFCs could be affected by a couple of factors including microbial inoculum, electrode materials, spacing, catalysts, types of reactors, substrates, operation conditions, and so on [7-10]. Among them, cathode was thought to be the greatest limiting factor toward future power improvement [2] compared with that of anode [11-13]. For instance, the maximum power density could reach  $6860\text{mW/m}^2$  when the area ratio of the cathode and the anode was 14:1 [14]. So, cathode was very important for MFCs to exhibit desired performance.

Up to date, various types of cathodes have been fabricated such as electrolytic cathode, biocathode and air cathode [15]. Air cathode was well developed due to the distinguishing features of reasonable cost and scalable for practical applications. "Sandwich type" framework is commonly designed for air cathode, whose detailed compositions (from air facing side to solution facing side) generally consisted of air diffusion layers, the matrix and catalyst layers [16, 17]. The main concerns of the air cathode were optimization of air diffusion layers and searching for substitutes of polytetrafluoroethylene (PTFE), screening of different metallic and non-metallic cathode materials [16-20], comparison of precious and non-precious catalysts [21-26], and application of different catalyst binders as well as their composites [27]. However, cathode catalyst support materials (CSMs) were scarcely paid too much attention.

The CSMs are the basic materials for supporting catalyst [28] [29]. It is recognized that the ideal CSM can provide high chemical stability, enough surface area, strong mechanical strength, and outstanding electrical conductivity [30]. Recently, according to the reports, carbon materials like carbon black [31], carbon paper [9] and graphite granules [32] were commonly used as the CSMs in the field of MFCs, and the nano materials including carbon nanotube (CNT) [33, 34] and graphene [20, 35] were applied as the CSMs as well. It was identified that the catalytic effect of catalyst could be enhanced through appropriate treatment with the CSMs. However, only few reports paid close attention to the functioning of CSMs in the field of MFCs [35-37].

CNT, which was discovered in 1991, is a relatively new type of carbon material. It has been considered to be a good CSM due to its unique properties including special tube structure and almost all characteristics of ideal CSM [38]. Consequently, CNT could be the potential CSM in MFCs. However, the superior chemical inertia also limited the use of CNT itself since the poor reactivity of CNT would result in the difficult adhesion of metallic catalyst particles. It was suggested that such situation could be resolved by chemical surface modification via strong oxidants such as nitric, sulfuric and mixed acid [39, 40].

Oxygen Reduction Reaction (ORR) is one of the most important part for the cathode performance in fuel cells, whose performance was increased with the improvement of the ORR efficiency [41, 42]. It was considered that ORR efficiencies could be increased by using catalysts for reduction of activation energy or by modifying CSMs. However, most of the studies paid attentions to the prior one. Catalysts such as special metals, metal complex, and metallic oxide have been applied widely since they could speed up the ORR [42, 43]. In fact, different CSMs could affect the dispersibility and homogeneity of the metallic particles in catalyst [44]. In this study, we selected the carboxylic CNTs under different conditions as the CSMs, prepared the Pt/CNT catalysts and tested

their efficiency of the ORR in MFCs. The results indicated that properly carboxylated CNT could serve as an excellent CSM. The aim of this study was to evaluate the effect of modified CNT under different conditions as the CSM on ORR at the cathode of MFC. X-ray photoelectron spectroscopy (XPS), X-ray diffraction (XRD) and scanning electron microscope (SEM) techniques were employed to analyze the properties of the prepared CSM of CNT and catalysts. Experiments of in situ electricity generation in MFCs were carried out to confirm the results.

## 2. MATERIALS AND METHODS

### 2.1. CSM, catalyst and cathode preparation

CNTs (S-MWNT-1030, Shenzhen Nano-Tech Port Co., Ltd., China) were modified with carboxylic group reacted under two different reflux systems. Accordingly, two kinds of CSMs were harvested. The preparation method of the first kind of CSM was as follows: the carboxylation of CNT was carried out in a mixture of nitric (70 wt.%) and sulfuric (96wt.%) acids at 80 °C (denoted as CNT-1). For the second one, the modification of CNT was accomplished with a nitric (70wt.%) and sulfuric (96wt.%) acids at 95 °C (denoted as CNT-2) [45]. Then, the treated CNTs were rinsed with deionized water until the pH was about 7.

Pt/CNT catalysts were prepared by dipping-precipitation method. The CNT-1 or CNT-2 was fully dispersed in the ethanol solution of chloroplatinic acid and stirred into slurry. Then, formaldehyde (37%) was added to the suspension to reduce platinum after the suspension was adjusted to alkalescence. Finally, the products were dried under vacuum [46]. The prepared catalysts were coated on the CNT-1 and CNT-2, which were denoted as Pt/CNT-1 and Pt/CNT-2, respectively.

Consequently, the cathodes were made by using the sandwich structure including catalyst layer, support, and diffusion layer (DL)/Waterproof layer. Titanium mesh (Anping Sheng Zhuo Mesh Products Co., Ltd., 100 meshes, wire diameter 0.1mm) was used as the support of cathode. On the air-facing side, four PTFE layers as the DL [9] were applied onto the Ti mesh which were washed in the 0.5mol/L H<sub>2</sub>SO<sub>4</sub>, acetone and deionized water in the ultrasonic bath successively. However, on the water-facing side, the prepared Pt/CNT-1 and Pt/CNT-2 (0.5mg/cm<sup>2</sup>) catalysts were dispersed with PTFE (5%) and brushed onto the support uniformly. The prefabricated cathodes were employed in the M80 and M95, respectively. The control group adopted Pt cathode and the same prepared PTFE diffusion layer was included.

### 2.2. Anode preparation

The anode materials were the carbon felts (CFs) (0.5cm thickness, 2.0cm diameter, Liaoyang Jingu Carbon Fiber Sci-Tech Co. Ltd., China). Before using, the CFs were pretreated and modified as previously reported [47]. Briefly, the CFs were soaked in acetone for 3h, boiled in deionized water for 6 times (the deionized water was changed every 0.5h), then modified in concentrated nitric acid for 5h, and washed by deionized water until pH was around 7.

### 2.3. Inoculants and acclimation

The inoculants in the MFCs were the sediment which was gathered from a local pond. Before the inoculants were used in the reactor, the sediment were acclimated by using artificial wastewater containing 1g/L glucose, 0.08g/L  $\text{NH}_4\text{Cl}$ , 0.04g/L  $\text{KH}_2\text{PO}_4$ , 0.48g/L yeast extract paste, and 5mL trace elements solution for at least 3days.

### 2.4. MFC configuration and operation

The membrane free single-chamber air cathode MFCs were constructed and the effective liquid volume was about 125mL, electrode spacing was 5cm, and electrode areas of cathode and anode were about  $12.56\text{cm}^2$ . the anode compartment was consisted of carbon felts. All reactors were operated in batch mode, inoculated with the mixtures of the nutrient medium and the supernatant of acclimated pond sediment (50%, v/v). The nutrient medium contains 1g/L glucose, 5mL/L vitamin solution, 12.5mL/L mineral solution and 50mmol/L PBS consisting of 0.31g/L  $\text{NH}_4\text{Cl}$ , 2.452g/L  $\text{NaH}_2\text{PO}_4 \cdot \text{H}_2\text{O}$ , 4.576g/L  $\text{Na}_2\text{HPO}_4$  and 0.13g/L  $\text{KCl}$  [48, 49]. During the whole operating period, the external resistor was maintained at  $1000\Omega$  except for the polarization curve determination. The reactor solution was not replaced until the voltage decreased to around 0.05V. All experiments were conducted at  $30^\circ\text{C}$  in the incubator. MFCs equipped with the cathodes prepared by Pt/CNT-1, Pt/CNT-2 and Pt/C as well as C were denoted as M80, M95 and MPT as well as MC, respectively.

### 2.5. Analysis and calculations

#### 2.5.1. XPS analysis

The surface elements and functional groups of the CNT-1, CNT-2 and untreated CNT were examined by, X-ray Photoelectron Spectroscopy (Axis Ultra DLD, Kratos Analytical Ltd., England) with a monochromatized Al  $K\alpha$  X-ray (Mono Al $K\alpha$ ) source ( $h\nu=1486.6\text{eV}$ ,  $10\text{mA}\times 15\text{KV}$ ), the beam spot size was  $700\times 300\mu\text{m}$ , and the style of the scanning was CAE. The vacuum degree in the analysis chamber was maintained at  $5\times 10^{-9}$  Torr. Survey spectra and region scans were collected using pass energy of 160eV and 40eV respectively with the rate of 1eV per step. All binding energies were referenced to the C1s neutral carbon peak at 284.6eV.

#### 2.5.2. XRD analysis

Pt/CNT-1 and Pt/CNT-2 were subjected to X-ray diffraction (XRD) analysis with a D8 ADVANCE X-ray diffractometer (Bruker, Germany) using Cu KR radiation ( $\lambda=0.15418\text{nm}$ ). The beam voltage and beam current settings were 40kV and 40mA, respectively. Samples were spread onto glass slides and scanned at  $0.2^\circ 2\theta \text{ s}^{-1}$ .

### 2.5.3. SEM tests

The surface morphologies of the Pt/CNT-1 and Pt/CNT-2 catalysts and untreated CNT were examined by a scanning electron microscope (S-3000N, Hitachi, Japan), operating at an accelerating voltage of 15kV to identify the surface characteristics and the deposited Pt particles.

### 2.5.4. Cell performance

The cell voltage ( $U$ ) and anode potential were recorded using a data acquisition system (2700, Keithly). Current density ( $A/m^2$ ) was calculated as  $I=U/(RS)$ , where  $S$  is the surface area of the anode ( $12.56cm^2$ ),  $R$  is the external resistance. Power density ( $mW/m^2$ ) was calculated as  $P=1000U^2/(RS)$  (1000 is used for unit conversion). Polarization Curves were plotted by varying the external resistance over a range from  $90000\Omega$  to  $20\Omega$  when the cell voltage was stable, repeatable and reached the platform period. The internal resistance ( $r$ ) was investigated using Steady state discharge method, which was measured by changing different external resistance. Afterwards, the slope of the polarization fitting equation was internal resistance.

## 3. RESULTS AND DISCUSSION

### 3.1. Effect of cathode prepared with different CSMs on power generation of MFCs

The cell voltage curves of M80, M95 and MPT (MPT was the control) as well as MC were exhibited in Fig.1. It showed that M80 and M95 were successfully activated since stable and repeatable voltages were obtained after 150h inoculation while MC cannot start up successfully due to the low voltage which failed to acquire more than 0.1V. During the whole operation of MFC, M80 took 928h to obtain the voltage of 0.43V, However, 662h was required for the M95 to reach 0.46V, which indicated that both the Pt/CNT-1 and Pt/CNT-2 could catalyze the ORR at the cathodes of MFCs effectively. Furthermore, the M95, equipped with cathode preparing by the Pt/CNT-2 which used CNT-2 as the CSM, showed higher ORR efficiency and shorter start-up period than those of M80. It implied that the prepared CSM CNT-2 was more effective than CSM CNT-1. However, the voltage output of MPT was attained at 0.336V around 1118h, which take much longer time to achieve the highest voltage than M80, M95, MC.

The polarization and power density curves of the three cells were shown in Fig.2. Fig.2 exhibited the open circuit voltages (OCVs) of M80 and M95 were 0.736V and 0.776V, respectively. It could have been found that the maximum power densities of M80 and M95 were  $773.9mW/m^2$  and  $911.3mW/m^2$ , both much greater than  $447.3mW/m^2$  for MPT (Fig.2).

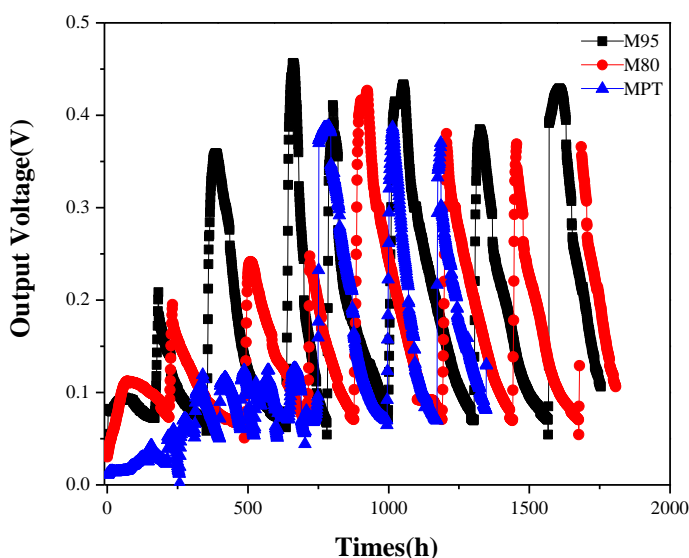


**Figure 1.** Start-up characteristics of M80, M95, and MPT

Similarly, the internal resistance of M80 and M95 were  $359\Omega$  and  $310\Omega$ ; from which both were lower as compared with that  $518\Omega$  of MPT. It is because the untreated CNT was inert, the introduction of O, N and S-containing groups on the surface of CNT can greatly enhance the hydrophilicity as well as the uniformity of Pt coated on CNT, thus increased the chemical active site [50, 51], which resulted in reduction of resistance and higher voltages and power densities. Moreover, voltage and power density of M95 were both superior to M80 at the same current density, which implied that the Pt/CNT-2 showed better catalytic performance than that of Pt/CNT-1. It demonstrated that the prepared CSM CNT-2 was better than CNT-1.

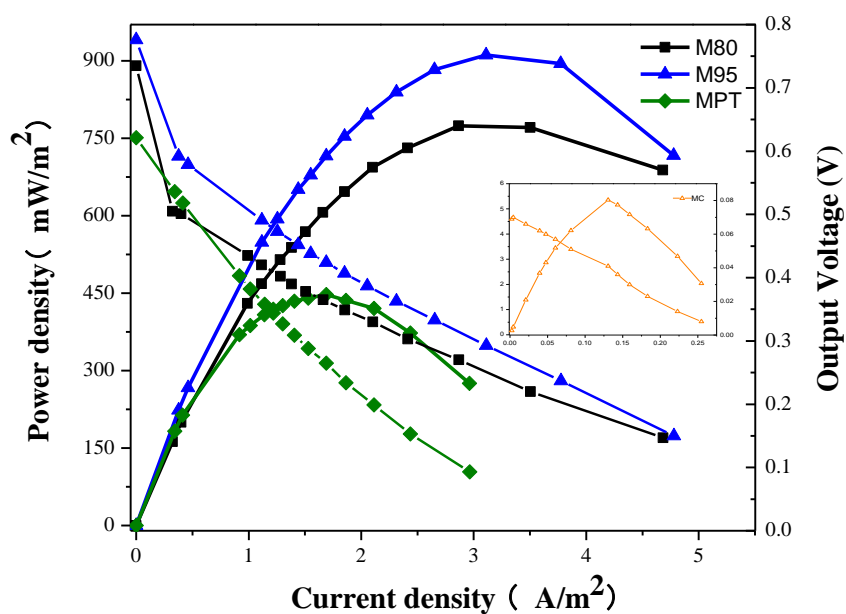


**Figure 2.** Polarization and power density curves of M80, M95, MPT and MC

### 3.2. The analysis of prepared CSMs and catalysts

#### 3.2.1. Catalyst support materials

In order to identify the difference of prepared CSMs in various carboxylic conditions, the CSMs CNT-1 and CNT-2 and untreated CNT (denoted as CNT-0) samples were performed for XPS analysis. The whole spectra and surface elemental content of the CNT-0, CNT-1 and CNT-2 were shown in Table 1 and supporting material, respectively. The results indicated that C and O were the mainly elements of the three CNTs. To the uppermost element C, the peak intensity of C1s of the CNT-0, CNT-1 and CNT-2 were decreased systematically, which indicated that carboxylation of CNT in the 95 °C reflux system was more completely than that in 80 °C reflux system. However, the contents of N and S were 0.7% and 0.32% for CNT-1, and 1.91% and 1.99% for CNT-2, respectively. It might due to that more N-containing groups and S-containing groups were introduced onto the surface of CNT-2 than CNT-1.

**Table 1.** Surface elemental content of the CNT-0, CNT-1 and CNT-2

Element	CNT-0	CNT-1	CNT-2
C1s (%)	94.11	93.37	85.08
O1s (%)	5.89	5.62	11.03
N1s (%)	0.00	0.70	1.91
S2p (%)	0.00	0.32	1.99
WC (%)	38.31	0.00	0.00
C–C/C–H (%)	43.42	57.95	52.82
C–OH (%)	4.11	12.02	14.56
C=O (%)	9.56	10.09	10.40
COOH (%)	4.60	19.94	22.23

The spectra about C1s of the untreated CNT-0 and CSMs CNT-1 and CNT-2 were exhibited in Fig.3. It showed that C1s spectra of the samples exhibited the maximum peak at binding energy (BE) about 284.6eV after calibration, which seemed to be the C–C/C–H peaks. The peaks at binding energy about 285.6eV, 286.7eV and 288.7eV were also displayed and could be identified as C–OH, C=O and COOH, respectively. Quantificationally, as shown in Table1, the contents of C–OH in the CNT-1 and CNT-2 were 12.02% and 14.56%, respectively, while only 4.11% in the untreated CNT-0. Meanwhile, in comparison with 4.6% for the CNT-0, the contents of COOH in the CSMs CNT-1 and CNT-2 were 19.94% and 22.23%, respectively. Actually, mixed acids reflux systems were widely used to increase O-containing groups of carbon materials[52]. It also revealed that more –OH and –COOH were generated under reflux system at 95 °C than those at 80 °C. Overall, the O-containing functional groups of CSMs CNT-1 and CNT-2 were more abundant than those of untreated CNT-0, which might be the active sites for Pt loadings including coordination, adsorption and replacement [50, 53].

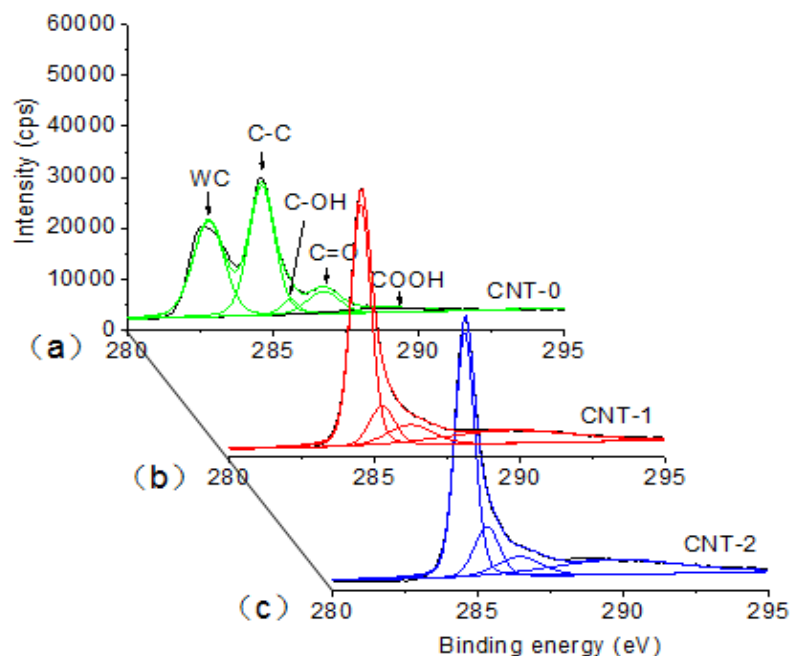


**Figure 3.** XPS spectra about C1s of CNT-0, CNT-1 and CNT-2

### 3.2.2. Pt/CNT-1 and Pt/CNT-2 catalysts

The generated CSMs CNT-1 and CNT-2 were subjected to prepare Pt/CNT-1 and Pt/CNT-2 catalysts by dipping-precipitation method, respectively. The Pt contents of the Pt/CNT-1 and Pt/CNT-2 catalysts were measured by combustion [50]. After calcinating at 800 °C about 10min, it could be calculated that the Pt contents of the Pt/CNT-1 and Pt/CNT-2 catalysts were both 11%. In order to verify the prepared Pt/CNT catalysts, SEM and XRD analysis were performed.

The SEM images of the untreated CNT, Pt/CNT-1 and Pt/CNT-2 catalysts were shown in supporting materials. The results exhibited that many Pt nanoparticles were evidently adhered on the walls and prots of CSMs CNT-1 and CNT-2 after dipping-precipitation. Additionally, the uniformity and dispersibility of Pt nanoparticles on CSM CNT-2 were better than those on CSM CNT-1.

The XRD patterns of Pt/CNT-1 and Pt/CNT-2 catalysts were shown in Fig.4. Generally, the XRD patterns of the prepared catalysts were similar. It could be found that there was an obvious sharp (002) plane at  $2\theta=26.1^\circ$  in both samples, which was considered to be the characteristic diffraction peak for C [54]. The other two peaks with less intense and asymmetrical reflection for C (100) and C (004) planes at  $2\theta$  to  $42.7^\circ$  and  $53.6^\circ$  were also presented. Comparing with Pt/CNT-1, the characteristic diffraction peak for C of Pt/CNT-2 was lower, which meant that the structure of C was carboxylated more thoroughly at 95°C reflux system than that at 80 °C. However, the XRD patterns for the characteristic reflections for Pt implied that the Pt particles in the prepared catalysts were the typical cubic surface structure [41, 55]. According to the half-peak width of the pattern (220), the average Pt particle size of the crystals could be calculated by Debye-Scherrer equation, which showed that the average Pt particle size of the prepared Pt/CNT-1 and Pt/CNT-2 catalyst was 30.4nm and 28.2nm, respectively. Comparing with Pt/CNT-1, the diffraction peaks for Pt of Pt/CNT-2 were higher,

especially the characteristic diffraction peak for Pt. It showed that Pt nanoparticles of Pt/CNT-2 catalyst had better defined crystals, more perfect crystalline forms, and smaller average sizes, which could provide more attachment between oxygen and Pt nanoparticles, and therefore, superior catalytic ORR performances were realized.

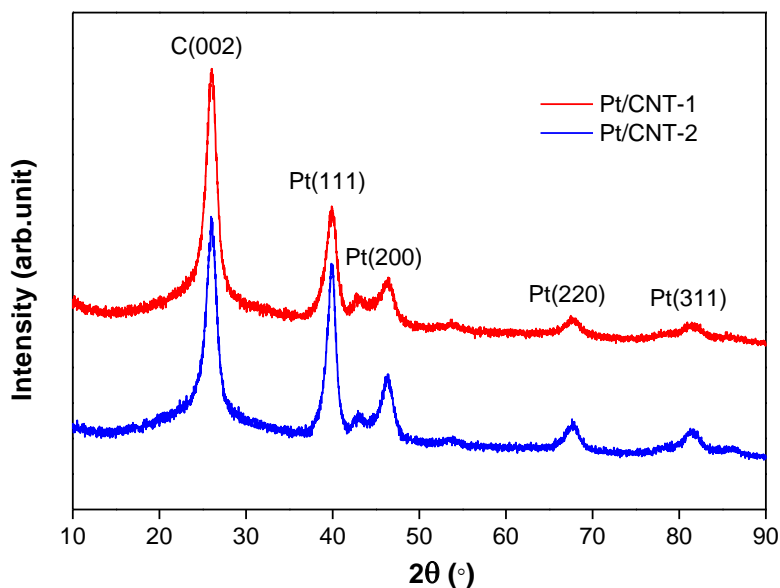


**Figure 4.** The XRD patterns of Pt/CNT-1 and Pt/CNT-2

### 3.3. The enhancement of ORR efficiency and its interpretation

ORR is the most important part for the cathode performance in fuel cells, whose performance was increased with the improvement of the ORR efficiency. It was considered that ORR efficiencies could be increased by using catalysts for reduction of activation energy or by modifying CSMs. However, most of the studies paid attentions to the prior one. In fact, different CSMs could affect the dispersibility and homogeneity of the metallic particles in catalyst. In this study, we selected the carboxylic CNTs under different conditions as the CSMs, prepared the Pt/CNT catalysts and tested their efficiency of the ORR in MFCs. The results indicated that properly carboxylated CNT could serve as an excellent CSM.

Furthermore, XPS analysis was adopted in CNTs and XRD, SEM analysis were applied in Pt/CNT catalysts to explore why CSM CNT-2 was better than CNT-1, respectively. It was revealed that the ORR efficiency of Pt/CNT-2 catalyst was superior than that of Pt/CNT-1 due to that more O-containing functional groups such as  $-OH$  and  $-COOH$  were generated on the surface of CNT-2 than that on CNT-1. The generated O-containing groups were beneficial to the dispersion and deposition of Pt particles on the CSMs as well as the enhancement of ORR efficiency. Furthermore, a few of N-containing groups and S-containing groups were also generated under the reflux systems. It was considered that the introduced S-containing groups (such as  $-SO_3H$ ) could act as the active sites for the deposition of the Pt particles in the replacement reaction of Pt reduction process [50]. Briefly, more

abundant O, N, and S-containing groups were introduced in carboxylic CNT-2, which provided more chemical activity sites for the enhancement of Pt homogenous dispersion.

Carboxylation is a common method for the surface modification of carbon materials. It has been reported in the field of methanol chemical fuel cells to enhance ORR efficiency. However, very few reports focused on the CSM carboxylation in the field of MFCs. For example, it was considered that the electrocatalytic performance of dissolved oxygen reduction for graphite granules at neutral pH in MFC could be increased via activation in 5% nitric acid reflux system. In fact, the CSMs could affect ORR performance. The ORR of commonly used CSMs like carbon black (i.e. Vulcan XC-72), graphite, and nanocarbon materials (i.e. CNT and graphene) could be improved by functionalization, for example, carboxylation. In this study, two kinds of carboxylic CNTs CSMs and catalysts were prepared and evaluated in MFCs. The results showed that the CSM CNT-2 prepared under 95°C reflux system was superior to CNT-1 prepared at 80°C, indicated that higher content of functional groups introduced resulted in more active sites of CNT-2 generated, smaller Pt particle size led to more dispersiveness of Pt/CNT-2 catalyst, and greater maximum power density gave rise to lower internal resistance of MFC-2. Afterwards, the outcome implied that the carboxylation of CSMs could be a feasible pathway to improve the performance of prepared catalysts and ORR efficiency of the cathode in MFCs. Besides, further work could be included in the optimization of carboxylic system such as concentration of acids, ratio of mixed acids, refluxing time, reaction temperatures, and more efficient approaches to treat catalyst as well.

#### 4. CONCLUSIONS

The Pt/CNT-1 and Pt/CNT-2 catalysts using carboxylic CNTs (CNT-1 and CNT-2) as CSMs were prepared and their ORR efficiencies were tested in air cathode MFCs (M80 and M95). In comparison with the control MPT, M80 and M95 had far superior performances in terms of higher maximum power densities, higher OCVs, lower internal resistances, and shorter start-up periods. Furthermore, the power density and output voltage of M95 were both higher than M80 in the same current density, which proved that the Pt/CNT-2 had better catalytic ORR efficiency than Pt/CNT-1. XPS, XRD and SEM analysis revealed that CNT which was treated in reflux system at 95 °C (CNT-2) introduced more abundant O, N, and S-containing groups than CNT-1 prepared at 80°C, which provided more chemical activity sites for the enhancement of Pt homogenous dispersion, resulting in more perfect crystalline forms of the Pt particles.

#### ACKNOWLEDGEMENTS

The authors would like to thank National Natural Science Foundation of China (30800796 and 31272482), Program for New Century Excellent Talents in University (NCET-11-0166), and the Fundamental Research Funds for the Central Universities (2014ZG015) for financial support.

## References

1. D.R. Bond and D.R. Lovley, *Appl. Environ. Microb.*, 69 (2003) 1548-1555
2. B.E. Logan, B. Hamelers, R. Rozendal, U. Schröder, J. Keller, S. Freguia, P. Aelterman, W. Verstraete and K. Rabaey, *Environ. Sci. Technol.*, 40 (2006) 5181-5192
3. K. Rabaey, N. Boon, S.D. Siciliano, M. Verhaege and W. Verstraete, *Appl. Environ. Microb.*, 70 (2004) 5373-5382
4. Y. Feng, Q. Yang, X. Wang and B.E. Logan, *J. Power Sources*, 195 (2010) 1841-1844
5. I.S. Chang, B.H. Kim, H.J. Kim, D.H. Park and P.K. Shin, *Google Patents*, 1999
6. Z. Li, X. Zhang and L. Lei, *Process Biochem.*, 43 (2008) 1352-1358
7. Y. Qiao, C.M. Li, S.J. Bao and Q.L. Bao, *J. Power Sources*, 170 (2007) 79-84
8. S. Cheng, H. Liu and B.E. Logan, *Electrochem. Commun.*, 8 (2006) 489-494
9. J.R. Kim, S.H. Jung, J.M. Regan and B.E. Logan, *Bioresour. Technol.*, 98 (2007) 2568-2577
10. Y. Fan, E. Sharbrough and H. Liu, *Environ. Sci. Technol.*, 42 (2008) 8101-8107
11. I.H. Park, M. Christy, P. Kim and K.S. Nahm, *Biosens. Bioelectron.*, 58 (2014) 75-80
12. Y.Q. Wang, B. Li, D. Cui, X.D. Xiang and W.S. Li, *Biosens Bioelectron.*, 51 (2014) 349-355
13. U. Karra, B.K. Li, S. Manickam and J. McCutcheon, *Abs. Pap. Acs.*, 243 (2012)
14. S. Oh, B. Min and B.E. Logan, *Environ. Sci. Technol.*, 38 (2004) 4900-4904
15. S. Cheng, H. Liu and B.E. Logan, *Environ. Sci. Technol.*, 40 (2006) 2426-2432
16. Y. Luo, F. Zhang, B. Wei, G. Liu, R. Zhang and B.E. Logan, *J. Power Sources*, 196 (2011) 9317-9321
17. I. Roche, K. Katuri and K. Scott, *J. Appl. Electrochem.*, 40 (2010) 13-21
18. G.G. Kumar, Z. Awan, K.S. Nahm and J.S. Xavier, *Biosens. Bioelectron.*, 53 (2014) 528-534
19. B.T. Li, X.X. Zhou, X.J. Wang, B.C. Liu and B.K. Liu, *J. Power Sources*, 272 (2014) 320-327
20. Z.H. Yan, M. Wang, B.X. Huang, R.M. Liu and J.S. Zhao, *Int. J. Electrochem. Sci.*, 8 (2013) 149-158
21. Y.Y. Jiang, Y. Xu, Q. Yang, Y.W. Cheng, S.M. Zhu and S.B. Shen, *Int. J. Energ. Res.*, 38 (2012) 1416-1423
22. M. Lu, L. Guo, S. Kharkwal, H.N. Wu, H.Y. Ng and S.F.Y. Li, *J. Power Sources*, 221 (2013) 381-386
23. M. Ghasemi, W.R.W. Daud, M. Rahimnejad, M. Rezayi, A. Fatemi, Y. Jafari, M. Somalu and A. Manzour, *Int. J. Hydrogen Energy.*, 38 (2013) 9533-9540
24. C.H. Wang, C.T. Wang, H.C. Huang, S.T. Chang and F.Y. Liao, *Rsc Adv.*, 3 (2013) 15375-15381
25. X.H. Li, N.W. Zhu, Y. Wang, P. Li, P.X. Wu and J.H. Wu, *Bioresour. Technol.*, 128 (2013) 454-460
26. L. Deng, H. Yuan and Y. Chen, *Eng. J. Wuhan Univ.*, 45 (2012) 703-707
27. C.W. Bezerra, L. Zhang, H. Liu, K. Lee, A.L. Marques, E.P. Marques, H. Wang and J. Zhang, *J. Power Sources*, 173 (2007) 891-908
28. I. Roche and K. Scott, *J. Electroanal. Chem.*, 638 (2010) 280-286
29. K. Lee, L. Zhang, H. Lui, R. Hui, Z. Shi and J. Zhang, *Electrochim. Acta.*, 54 (2009) 4704-4711
30. L. Deng, M. Zhou, C. Liu, L. Liu, C. Liu and S. Dong, *Talanta*, 81 (2010) 444-448
31. Y. Yuan, S. Zhou and L. Zhuang, *J. Power Sources*, 195 (2010) 3490-3493
32. S. Freguia, K. Rabaey, Z. Yuan and J. Keller, *Electrochim. Acta.*, 53 (2007) 598-603
33. H.Y. Tsai, C.C. Wu, C.Y. Lee and E.P. Shih, *J. Power Sources*, 194 (2009) 199-205
34. G.M. Yang and F.Q. Zhao, *Biosens. Bioelectron.*, 64 (2015) 416-422
35. J. Wu, Y. Wang, D. Zhang and B. Hou, *J. Power Sources*, 196 (2011) 1141-1144
36. E. Yoo, T. Okada, T. Akita, M. Kohyama, I. Honma and J. Nakamura, *J. Power Sources*, 196 (2011) 110-115
37. G. Che, B.B. Lakshmi, C.R. Martin and E.R. Fisher, *Langmuir*, 15 (1999) 750-758

38. J. Planeix, N. Coustel, B. Coq, V. Brotons, P. Kumbhar, R. Dutartre, P. Geneste, P. Bernier and P. Ajayan, *J. Am. Chem. Soc.*, 116 (1994) 7935-7936
39. M.J. O'Connell, P. Boul, L.M. Ericson, C. Huffman, Y. Wang, E. Haroz, C. Kuper, J. Tour, K.D. Ausman and R.E. Smalley, *Chem. Phys. Lett.*, 342 (2001) 265-271
40. H. Yu, Y. Jin, F. Peng, H. Wang and J. Yang, *J. Phys. Chem. C.*, 112 (2008) 6758-6763
41. I. Roche, E. Chaînet, M. Chatenet and J. Vondrák, *J. Appl. Electrochem.*, 38 (2008) 1195-1201
42. S. Guo, L. Wang, S. Dong and E. Wang, *J. Phys. Chem. C.*, 112 (2008) 13510-13515
43. M. Lu, S. Kharkwal, H.Y. Ng and S.F.Y. Li, *Biosens. Bioelectron.*, 26 (2011) 4728-4732
44. L. Gan, H.D. Du, B.H. Li and F.Y. Kang, *New Carbon Mater.*, 25 (2010) 53-59
45. C.H. Feng, L.M. F.B. Li, H.J. Mai, X.M. Lang, S.S. Fan, *Biosens. Bioelectron.*, 25 (2010) 1516-1520
46. H. Liu and B.E. Logan, *Environ. Sci. Technol.*, 38 (2004) 4040-4046
47. Y. Yuan, B. Zhao, S. Zhou, S. Zhong and L. Zhuang, *Bioresour. Technol.*, 102 (2011) 6887-6891
48. D.R. Lovley and E.J. Phillips, *Appl. Environ. Microb.*, 54 (1988) 1472-1480
49. M. Peuckert, T. Y, R.A.D. Betta, M. Boudart, *J. Electrochem. Soc.*, 133 (1986) 944-947
50. A. Ocampo, M. Miranda-Hernandez, J. Morgado, J. Montoya and P. Sebastian, *J. Power Sources*, 160 (2006) 915-924
51. Y. C. Xing, *J. Phys. Chem. B.*, 108 (2004) 19255-19259
52. D.T. Colbert and R.E. Smalley, *Trends Biotechnol.*, 17 (1999) 46-50
53. B.C. Satishkumar, E. Vogl, A. Govindaraj and Rao.C, *J. Phys. D. Appl. Phys.*, 29 (1996) 3173-3176
54. Z.Q. Tian, S.P. Jiang, Y.M. Liang and P.K. Shen, *J. Phys. Chem. B.*, 110 (2006) 5343-5350
55. G. Wu and B.Q. Xu, *J. Power Sources*, 174 (2007) 148-158